Spacer-Controlled Aggregation and Surface Morphology of a Selenacarbocyanine Dye on Gemini Monolayers

Guocheng Zhang, Xiaodong Zhai, and Minghua Liu*

Beijing National Laboratory for Molecular Sciences (BNLMS), CAS Key Laboratory of Colloid and Interface Science, Institute of Chemistry, CAS, Beijing 100080, P. R. China

Received: January 21, 2006; In Final Form: April 7, 2006

The adsorption and aggregation of a selenacarbocyanine dye (3,3-disulfopropyl-9-methyl-selenacarbocyanine, SeCy) onto Langmuir monolayers of a series of gemini amphiphiles with different methylene spacers were investigated. When the monolayers of the gemini amphiphiles were spread on the dye-containing subphase, the dye could be easily adsorbed and aggregated onto the monolayers through the electrostatic and $\pi-\pi$ interaction. The dye formed complexes with gemini amphiphiles and stacked as J-aggregates in all the transferred multilayers, regardless of the structure of gemini amphiphiles. However, the surface morphologies of the complex monolayers showed a significant dependence on the spacer length of the gemini amphiphiles and the temperature of the subphase. Nanorods were observed for the complex films with spacer lengths ranged from 4 to 10 methylenes. With the temperature of the subphases increased from 20 °C to 30 °C, aligned longer nanofibers were formed instead. Although both the gemini amphiphiles and the dye were achiral, strong circular dichroism (CD) signals were observed for the transferred complex films. However, the CD signals could be just opposite in different places of the transferred films, suggesting that a resolved enantiomeric micro/nanostructure coexisted in the films. On the other hand, for the complex film of the dye with the gemini amphiphile of two methylenes spacer, neither CD signal nor ordered surface morphologies were detected in any place of the film although the dye itself stilled formed J-aggregate in the film. It was suggested that regular nanoarchitectures and resolved chiral domains could be observed only when the spacer of gemini amphiphiles is comparative to the distance between the two SO_3^- groups in the dye.

Introduction

Cyanine dyes, as well as related thiacarbocyanine and selenacarbocyanines, can form J-aggregates that exhibit a sharp intense narrow absorption band at a wavelength longer than that of the monomer band under certain conditions.[1] Since its discovery by Jelly[2] and Scheibe,[3] much attention has been paid to the J-aggregate from their structural features,[4−7] photographic process[8,9] nonlinear optical properties,[10,11] and multiple wavelength optical recording materials.[12]

J-aggregates of cyanine dyes have been assembled in aqueous solutions,[2,3] in silver halide emulsions,[13,14] in solutions containing polyelectrolyte or salt,[15,16] and in films.[17−20] Since the J-aggregate is generally regarded as resulting from the interaction of large numbers of molecules in an orderly array, monolayer and Langmuir−Blodgett techniques, which provide excellent ways of controlling molecular arrangement,[21,22] have been widely used for the study of two-dimensional aggregation of dyes.[23−34] Besides the utilization of amphiphilic cyanine derivatives,[23−29] which are usually difficult to synthesize, the adsorption of water-soluble dye onto the organized molecular films is an easy way to fabricate the J-aggregates.[30−36] Using the Langmuir−Blodgett technique, not only can the aggregation be controlled in a two-dimensional way, but the surface morphologies of the film, which are also very important to the film properties, can also be regulated. Many interesting morphologies, such as leaflike islands,[37] polygonal domains,[36a] and "butterfly" or "spherulite" structures,[35c] have been reported. Great efforts have been devoted to the regulation on the aggregation and surface morphologies of the dyes in the organized molecular films using various kinds of amphiphiles. For example, typical amphiphiles which contain one headgroup and one or two alkyl chains such as dioctadecyldimethylammonium bromide (DODAB), octadecylammonium chloride (ODACl), arachidic acid (AA), and dihexadecyl phosphate (DHP) were mostly used.[32−36] Differently, here we report the control of the aggregation and surface morphologies of a selenacarbocyanine dye using gemini amphiphile monolayers.

Gemini amphiphiles, consisting of two amphiphiles covalently linked by a spacer between the two headgroups, possess tunable molecular geometry, unique aggregation property in aqueous solution, and superior performance in gene delivery.[38−41] So far, most of the research on the gemini amphiphiles has been focused on the solution system although there are some reports on the interfacial film systems. Our group has also reported a series of the work on the interfacial behaviors of the gemini amphiphiles with DNA,[42] water-soluble tetrakis(4-sulfonatophenyl)porphine (TPPS),[43] and polyoxometalate.[44] In this paper, we further extended the work to the control of the aggregation of the dye by the gemini amphiphiles with a continuously changeable spacer. We found that the spacer of the gemini could control both the aggregation and the surface morphologies of the formed complex films. In addition, the formed complex between the dye and the gemini amphiphiles showed enantiomeric chiral domains although both the gemini and dye were achiral.

The aggregation of the dye on the monolayers was studied by the surface pressure−area isotherms, and the transferred

* Author to whom correspondence should be addressed. Tel: +86-10-82612655; fax: +86-10-62569564; e-mail: liumh@iccas.ac.cn.

10.1021/jp060443a CCC: $33.50
Published on Web 05/10/2006

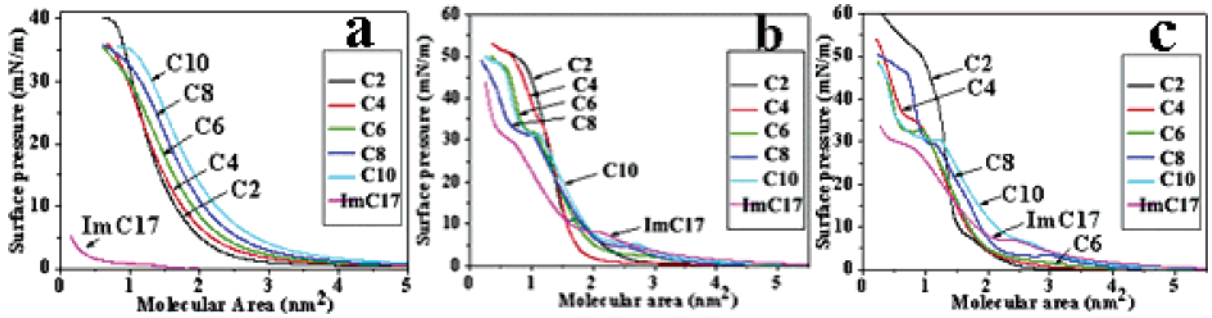

Figure 1. Surface pressure−area ($\pi-A$) isotherms of the monolayers of ImC17Cn ($n = 2, 4, 6, 8, 10$) and ImC17 spread on plain water (a) and those on the 2×10^{-6} M aqueous dye solution at 20 °C (b) and 30 °C (c), respectively. In the figure, Cn represents the corresponding ImC17Cn.

SCHEME 1. Molecular Structures and the Abbreviations of the Compounds Used in This Work

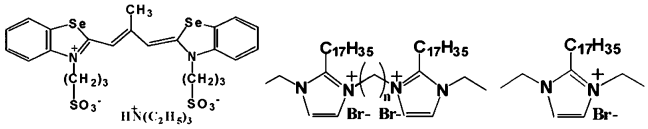

multilayer films were investigated using UV−vis spectroscopy, CD spectroscopy, and atomic force microscopy (AFM) measurement.

Experimental Section

Materials. The molecular structures of the amphiphiles and the selenacarbocyanine dye used in this work are shown in Scheme 1. The synthesis of the gemini amphiphiles is reported elsewhere.[43] The dye was purchased from Nippon Kankosikiso. In addition, we synthesized a conventional amphiphile having the same headgroup as the gemini amphiphiles, ImC17, as shown in Scheme 1, and compared its interfacial properties with those of the gemini amphiphiles.

Procedures. The aggregation of the dye SeCy on the gemini monolayers was performed on a KSV trough (KSV 1100, Helsinki, Finland). The gemini amphiphiles in chloroform solutions (ca. 0.1 mM) were spread on the aqueous subphase containing the dye, and the surface pressure (π)−molecular area (A) isotherms were recorded on a KSV minitrough. A concentration of 2×10^{-6} M was used because the dye existed as a monomer in this concentration. After 15 min for the evaporation of the solvent and the adsorption of the dye, surface pressure−area isotherms were recorded by compressing the barrier at a constant speed of 7.5 cm^2/min. The complex monolayers of the gemini amphiphiles and the dye were transferred onto quartz substrates by using a horizontal lifting method for UV−vis and CD measurements. CD spectra were recorded on a JASCO J-810 CD spectrometer. In the process of measuring CD spectra, the multilayer films on the quartz plates were placed perpendicular to the light path and were continuously rotated within the film plane, using a homemade attachment to avoid the possible linear dichroism (LD) in the films.[45,46] UV−vis spectra were recorded on a JASCO V-530 UV−vis spectrometer.

To measure the AFM of the transferred films, a freshly cleaved mica was used and AFM was recorded on a Digital Instruments Nanoscope IIIa (Santa Barbara, CA) with a silicon cantilever, using the tapping mode. AFM images are shown in the height mode without any image processing except flattening.

Results and Discussions

Aggregation of the Dye on Gemini Monolayers at the Air−Water Interface. Figure 1 shows the surface pressure−area ($\pi-A$) isotherms of the monolayers of the gemini amphiphiles on the water surface and the aqueous subphase containing 2×10^{-6} M dye at 20 °C and 30 °C. There is a clear difference between the monolayers on the water surface and the aqueous dye subphase. In the isotherms of the gemini/SeCy monolayers, clear transition regions are observed. It is further observed that depending on the spacer length of the gemini amphiphiles, there are one or two transition regions in the $\pi-A$ isotherms of gemini/SeCy monolayers. The surface pressure of the first transition region shows a dependence on the spacer length of the gemini amphiphiles, while the surface pressure at the second transition region is very similar regardless of the spacer lengths, which appears almost at the same surface pressure around 32 mN/m for all the gemini films. The monolayer of ImC17C2/SeCy is an exception, in which only one transition at 12mN/m was observed. This implies that the complex film of ImC17C2/SeCy might be different from those of the other gemini amphiphile with the dye.

TABLE 1: The Liftoff and Limiting Molecular Area of the Monolayers of the Gemini Amphiphiles on Different Subphases[a]

	water		SeCy (20 °C)		SeCy (30 °C)	
subphase	liftoff area	limiting area	liftoff area	limiting area	liftoff area	limiting area
ImC17C2	5.15	1.71	3.54	1.68	2.66	1.55
ImC17C4	5.87	1.97	3.10	1.75	3.27	1.89
ImC17C6	5.87	2.23	4.03	2.0	3.90	1.99
ImC17C8	6.02	2.33	4.03	2.18	4.16	2.24
ImC17C10	7.61	2.46	4.82	2.18	4.89	2.40
ImC17	1.48		5.14	1.94	5.18	2.27

[a] Unit: nm^2/molecule.

Second, both the liftoff area, which is the area where the surface pressure first appears, and the limiting molecular area, extrapolated from the linear part of the isotherm, showed a great change. For clarity, Table 1 listed a comparison of the corresponding data. It is clear that both the liftoff area and limiting molecular area decreased when the amphiphiles were spread on the dye subphase. Since the gemini amphiphiles are positively charged and SeCy has a net negative charge, it is reasonable to think that an electrostatic attraction cause the amphiphiles and dye to form the complex monolayers. The adsorption of negatively charged SeCy molecules will decrease the electrostatic repulsion among charged amphiphiles. Consequently, more condensed and stable complex films between the geminis and the dye, in which the dye was suggested to be mainly underneath the monolayer, were formed. With the spacer length increased, the molecular area showed an increase. However, the increase was not linear to the increase of the spacer length. This was due to the possible conformational change when the hydrophobic spacer was longer, which may be curved upward on water surface.[42,43] When the temperature of the

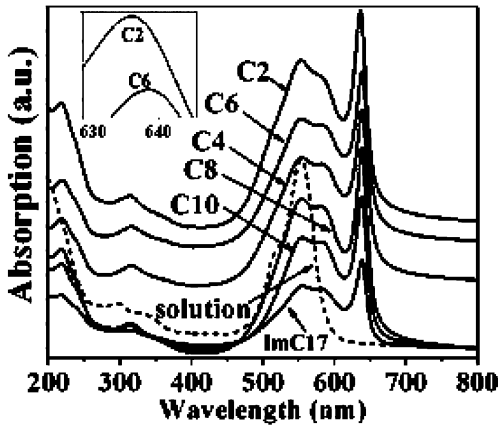

Figure 2. UV−vis spectra of the complex films of SeCy with different gemini amphiphiles ImC17Cn ($n = 2, 4, 6, 8, 10$) and ImC17 transferred at 15 mN/m and that of the SeCy aqueous solution, respectively. The inset is the expanded J-band around 640 nm.

subphase was increased to 30 °C, the essential shape and change tendencies with the spacer length of the isotherms were similar to those at 20 °C although the values of the liftoff and limiting molecular areas were slightly different.

On the other hand, while ImC17 itself did not form a stable monolayer, which may be because of the strong hydrophilicity of the headgroup, it formed a stable monolayer when spread on the dye. However, both the liftoff and limiting area of the monolayers on the dye subphase are similar to those of the gemini amphiphiles. Since the gemini amphiphile has two headgroups and ImC17 has only one, these values implied that more dye penetrated into the ImC17 monolayer than those of the gemini amphiphiles.

Characterization of the Transferred Complex Multilayer Films. The complex monolayers could be transferred onto solid substrates, and their spectral properties were characterized by UV−vis spectroscopy. Although both a vertical dipping and horizontal transfer could be applied to the film fabrication, the horizontal transfer was more effective in fabricating the multilayer films. A linear increase of the absorption spectra with the layer numbers was obtained during the fabrication of the multilayer films using the horizontal lifting method (see Supporting Information Figure S4). In addition, the same UV−vis spectra were obtained for the films fabricated in either way. To characterize the film with good resolution, we fabricated the multilayer films using a horizontal transfer method. Figure 2 gives the absorption spectra of the gemini/dye complex films transferred at 15 mN/m. In comparison, the absorption spectrum of the dye in the subphase was shown also. In the aqueous subphase, SeCy shows an intense absorption at 556 nm, which could be attributed to the monomer band. A new narrow, red-shifted absorption band was observed in the transferred complex films, which can be ascribed to the J-band of the dye. The appearance of this new band clearly suggested that through electrostatic interactions with the oppositely charged gemini monolayers, the dye molecules were orderly arranged to form the J-aggregate. In addition, a weak shoulder was detected at 584 nm, which is related to the absorption of dimer or oligomer. The J-band positions in all the gemini/dye films are observed at 639 nm, except for ImC17C2/dye, in which the band appeared at 636 nm. Since the position of the J-band is related to the size of the aggregates,[47] the lower wavelength of the J-band in ImC17C2/dye indicated that a small aggregate might be formed for ImC17C2/dye.

Morphological Investigation of the Transferred Complex Films. AFM is a powerful technique to get the information on surface morphology. It is particularly useful for the flat LB films. One layer of the complex monolayers of ImC17Cn/dye was deposited on the mica surface and its AFM was measured. Because the monolayers showed different transition pressures, every complex monolayer was transferred at different stages of the isotherms during the compression. Figure 3 shows the example of ImC17C10/SeCy monolayers transferred at different pressures. At a surface pressure of 3 mN/m, which is before the first plateau, a flat film with many holes is observed, as shown in Figure 3a. The height of the hole is about 1.22 nm. When the monolayer was compressed to 5 mN/m, a pressure above the first plateau, a lot of nanorods were observed. The nanorods can be extended to several micrometers. The enlargement of the nanorod indicated that these nanorods are composed of many clusters. The average height of the nanorod is about 1.42 nm. Further compressing the monolayer to 15 mN/m, which is between the first and the second transition region, the nanorods packed densely. In a certain region, the nanorods are aligned relatively regularly. When the film was further compressed near or up to the second plateau at 32 mN/m, the nanorods became more densely packed. In addition, some small domains appeared on the surface of the nanorod, indicating the collapse of the complex monolayers at this region. These morphological changes indicated that in the isotherms of monolayers of geminis/SeCy, the first plateau region was the transition from a liquid expanded phase to a condensed phase, while the second plateau indicated a transition from a condensed monolayer to a collapse film.

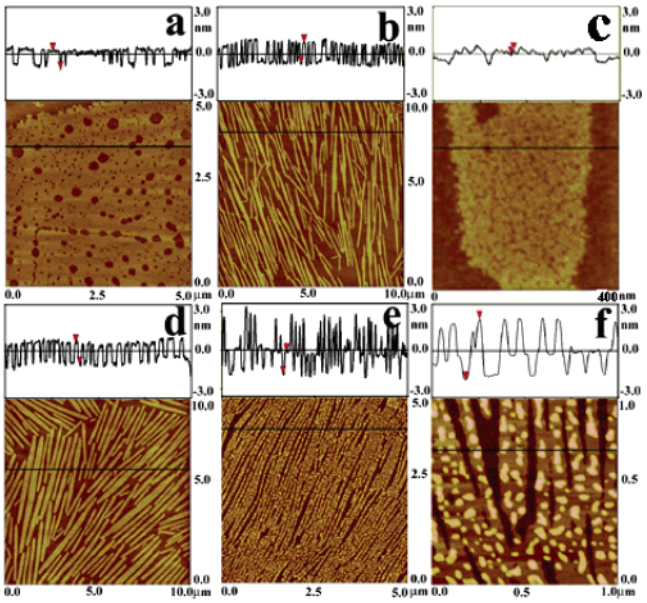

Figure 3. AFM images of the complex film of ImC17C10 spread on 2×10^{-6} M SeCy aqueous solution transferred at the pressures of (a) 3 mN, (b) 5 mN, (d) 15 mN, and (e) 30 mN. The AFM pictures in Figure 3c and 3f are the enlarged pictures of 3b and 3d, respectively.

A similar change of the AFM images was observed for the other complex films of ImC17Cn/SeCy ($n = 4, 6, 8, 10$) during the compression. Below the surface pressure of the first transition, flat films with some holes were observed. In the region between the first and the second plateau surface pressures, basically nanorods were found in all the complex films, as shown in Figure 4. Depending on the spacer length of the gemini amphiphile, the shape and size of the nanorod could be different. For the complex monolayer of ImC17C4/SeCy, rotted woodlike morphologies were observed. The side of the domains was quite rough. For ImC17C6/SeCy monolayer, a nanorod with nearly uniform width was observed. When the spacer length of the

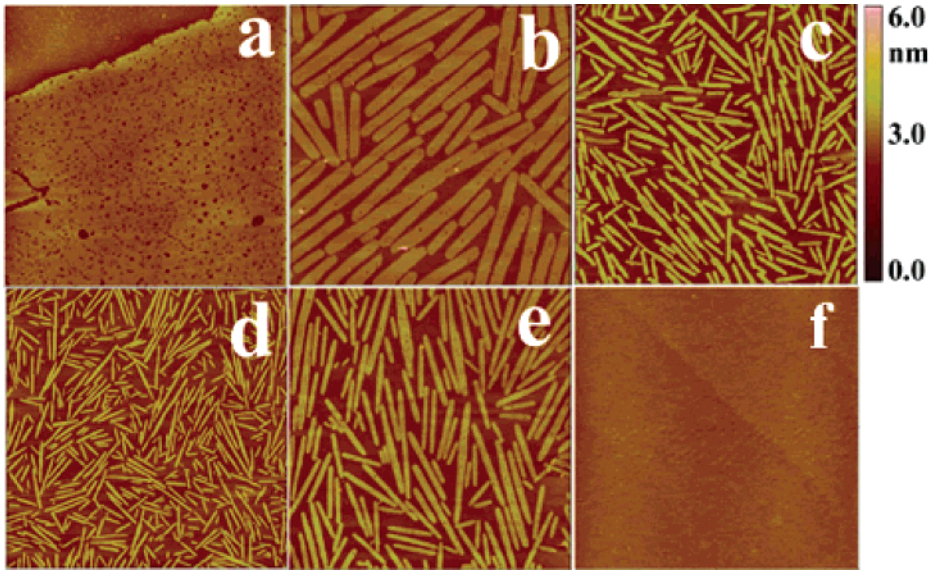

Figure 4. AFM images of the complex film of SeCy with (a) C2, (b) C4, (c) C6, (d) C8, and (e) ImC17 transferred at 15 mN/m at 20 °C and that of Gemini amphiphiles transferred from plain water (f) at 15 mN/m, respectively. All the images above are 10 μm × 10 μm in size.

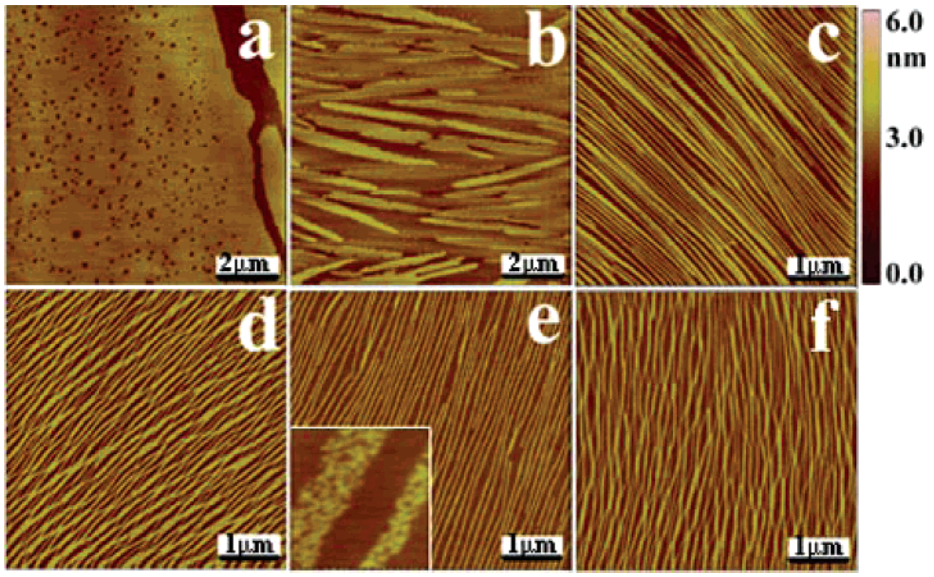

Figure 5. AFM images of the complex film of ImC17Cn/SeCy. (a) $n = 2$, (b) $n = 4$, (c) $n = 6$, (d) $n = 8$, (e) $n = 10$, and (f) ImC17 transferred at 15 mN/m at 30 °C. The inset of Figure 5e is the amplifying picture of the nanofiber the size of 250 nm × 250 nm.

gemini amphiphile was further increased, the width of the nanorod decreased. The thinnest nanorod was observed for ImC17C8/SeCy monolayer. For the complex film of ImC17C2/SeCy, only a larger flat domain with many holes was obtained. Neither nanorods nor blocks were observed. In addition, similar morphologies as shown in Figure 4a were obtained for the ImC17C2/dye monolayer, regardless of the surface pressures.

On the other hand, when the temperature of the subphase was increased, although the formed aggregates did not show any change in the UV−vis spectra, significant changes were observed in their morphologies. Figure 5 shows the AFM pictures for the complex films transferred at 15 mN/m. No obvious morphological change is detected for the monolayer of ImC17C2/SeCy. However, nanofibers were essentially formed instead of the nanorod for the other gemini/SeCy monolayers. The nanofibers can be extended to several tens of micrometers. In addition, these nanofibers are aligned in a certain direction, which seemed to be parallel to the dipping direction, although the nanofibers are basically curved. In some places, these nanofibers can be cross-linked. The enlargements of the nanofiber indicated that one nanofiber was composed of many aggregates.

Supramolecular Chirality of the Transferred Films. It has been reported that some achiral cyanine or porphyrin derivatives, when forming the J-aggregates in solution, could form chiral J-aggregates under stirring in one direction.[48,49] It was suggested that a helical stacking of the molecules formed the supramolecular chirality of the J-aggregates.[49] Previously, we had also found that a water-soluble TPPS could form chiral assemblies with some cationic amphiphiles in the organized molecular films.[50] Here, we have measured the CD spectra of the transferred gemini/dye films to see if the complex films have a supramolecular chirality or not.

Figure 6 shows the CD spectra of the ImC17C10/SeCy multilayer films. Positive and negative Cotton effect was observed with two crossovers at 584 nm and 638 nm, suggesting an exciton couplet type Cotton effect in the J-band.[51] In addition, in the monomer band, a conventional Cotton effect was observed

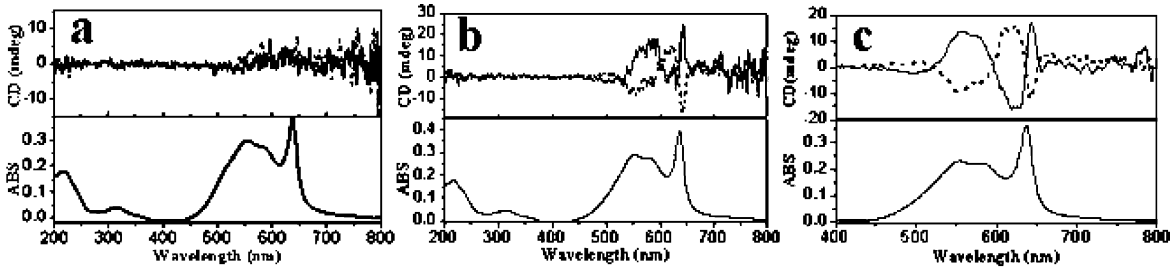

Figure 6. CD spectra of the complex films of ImC17Cn/SeCy (a) $n = 2$ and (b) $n = 10$ transferred at 15 mN at 20°C and (c) $n = 10$ transferred at 15 mN 30 °C.

at 554 nm. The exciton couplet and the monomer band are in the same sign. Although both the gemini amphiphiles and the dye were achiral, the formed multilayer complex films showed CD signals. This phenomenon is almost the same as our previous amphiphile/TPPS system. However, when we measured the CD spectra in different places of the film, the Cotton effect with just an opposite sign was observed. This phenomenon is completely different from our previously found TPPS/amphiphile films, in which different signs were observed in different fabrication batches. In the present case, different signals were observed in the film in the same run. This indicated that achiral molecules can also self-assemble into chiral domains as 2D conglomerates[52] or chiral racemates.[53,54]

We have carefully measured CD spectra in more than 20 places within a film. It was observed that the average of the whole film was nearly zero.

In the case of ImC17C2/SeCy, however, no CD signals can be observed in any place of the complex film. This suggested that no chiral domains formed in the film or that the chiral domain sizes were smaller than the beam size.

Discussion

The Langmuir−Blodgett technique provides a powerful method to control the molecular arrangement in two-dimensional air/water or air/solid interfaces. In the present case, the dyes could easily adsorb on the gemini monolayers through the electrostatic interaction and the $\pi-\pi$ stacking between the dye molecules. Because of the organization at the air/water interface, a small amount of the dyes could be mobilized onto the monolayer to form J-aggregates although such concentration is not sufficient for the dye to form J-aggregates in aqueous solution. These phenomena are essentially the same as those reported for the DODAB/cyanine systems. In the present case of gemini amphiphiles, however, the charge density and the distance between the two charge centers were precisely separated by a hydrophobic spacer. Such a spacer showed an obvious control on the aggregation and morphologies of the selanacarbocyanien dye. Because the main interaction between the geminis and the dyes could be electrostatic interaction, such control can be ultimately explained by the match between the distance of charge centers of the gemini amphiphile and the distance between the two negative headgroups in the SeCy.

According to the CPK models, the distances between the two positively charged ammonium groups are estimated to be 0.38, 0.63, 0.89, 1.14, and 1.40 nm for ImC17C2, ImC17C4, ImC17C6, ImC17C8, and ImC17C10, respectively, assuming that the alky chain is parallel to the water surface. On the other hand, the dye is a rigid molecule and can be regarded as a brick. The net charge of SeCy is negative. The distance of the two SO^{3-} end groups, which have the largest negative charge density, is about 0.65 nm. On the basis of this data, it is clear that the distance between the two charge centers in ImC17C2

SCHEME 2. Possible Interaction Mode for SeCy with C2 and Other Geminis

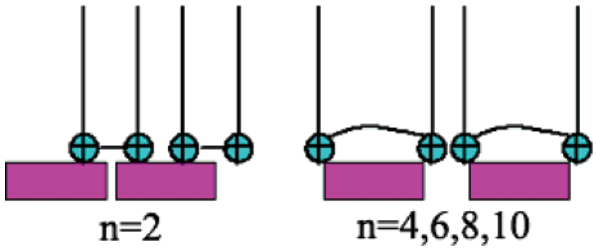

is obviously smaller than that of the dye and there existed a mismatch between ImC17C2 and the dye, as shown in Scheme 2. Therefore, we have observed in the UV−vis spectra that the J-band of ImC17C2/dye is a little blue shifted in comparison to that in the other gemini/dye films. In addition, because of the mismatch of the spacer length and the dye size, no ordered structure in a micrometer scale could be observed. For ImC17C4, the spacer length is close to that of the dye. The best match was realized formed for ImC17C4/dye. For the geminis with larger spacers, the hydrophobic alkyl spacer could be curved and the match could also be realized.[42] Consequently, it is reasonable to comprehend that the aggregation of cyanine dye in the complex films with ImC17C10, ImC17C8, and ImC17C6 is similar to that with ImC17C4 monolayer.

On the other hand, for ImC17, the distance between the headgroups was not fixed and a match can be realized in any case; therefore, we also observed the regularly arranged morphologies. No similar nanorods or nanofiber structures were observed in the conventional amphiphile/cyanine monolayers so far. In addition, different morphologies were observed when the present SeCy adsorbed on the monolayer of a conventional amphiphile such as CTAB (see Supporting Information). This suggested that the headgroup may affect the surface morphologies of the formed amphiphile/SeCy complex films although further investigation is needed.

Although both the gemini amphiphiles and the dye were achiral in solution, the formed complex films showed supramolecular chirality. Previously, we have found that the interfacially organized TPPS/amphiphile films showed similar chirality. It was suggested that a stacking of the TPPS rings in a helical sense caused the chirality. However, there is a clear difference between the TPPS/amphiphile and SeCy/gemini films in relation to the supramolecular chirality. In the case of TPPS, we got the CD signals with the same sign in any place of the film (film size was 1×3 cm^2). However, the sign of the Cotton effect could be just opposite for the film fabricated in different batches. In the present case of SeCy, we got the mirror CD signals in different places of the same film. Moreover, if we average the CD signals measured in different places of the film, then we can get zero signals. This indicated that at the present case, the chiral aggregate was resolved in a microscale in the film. The

difference between TPPS and SeCy J-aggregate film may be ascribed to their geometry. TPPS, as a square one, seems to be developed more continually than the rectangular SeCy dye in a two-dimensional way.

Conclusion

A water-soluble selenacarbocyanine dye can be adsorbed onto a series of gemini monolayers through the electrostatic interaction between the dye and the gemini amphiphiles and the $\pi-\pi$ stacking of the dyes. The SeCy molecules existed as J-aggregates in the complex monolayers because of the ordered arrangement of the dye in the monolayer and LB films. The formed complex films showed interesting morphologies such as nanorod and nanofiber, which are spacer- and temperature-dependent. Nanorods formed at a low temperature, while nanofibers shaped at a higher temperature. The thickness of the nanorod showed a change on the spacer length. The thinnest nanorod or nanofiber was formed for C8/SeCy film. The complex films showed local chirality although both the amphiphiles and dye were achiral. The gemini amphiphile with spacer length of C2 showed an exception. It formed J-aggregates, which showed a blue-shifted J-band in comparison with other gemini amphiphiles. No ordered nanoarchitecture in any temperature or surface pressure was observed. In addition, it never shows any chirality. Such regulation of the aggregation and the surface morphologies as well as the chirality of the dyes could be explained by the match between the size of the dye and the spacer distance in the gemini amphiphiles.

Acknowledgment. This work was supported by the National Natural Science Foundation of China (Nos. 20533050 and 90306002), the Basic Research Development Program (2005CCA06600), and the Fund of the Chinese Academy of Sciences.

Supporting Information Available: CD spectra of ImC17Cn/SeCy (n = 4, 6, 8) and the ImC17C2/SeCy complex film; surface pressure−molecular area isotherm, UV−vis and CD spectra, AFM images of CTAB/SeCy complex films. This material is available free of charge via the Internet at http://pubs.acs.org.

References and Notes

(1) Sturmer, D. M. In *Special Topics in Heterocyclic Chemistry*; Weissberger, A., Taylor, E. C., Eds.; Wiley: New York, 1977; Chapter 8.
(2) Jelly, E. E. *Nature* (London) **1936**, *138*, 1009; **1937**, *139*, 631.
(3) Scheibe, G. *Angew. Chem.* **1936**, *49*, 563; **1937**, *50*, 212.
(4) Cooper, W. *Chem. Phys. Lett.* **1970**, *7*, 73.
(5) Daltrozzo, E.; Gschwind, K.; Haimerl, F. *Photogr. Sci. Eng.* **1974**, *18*, 441.
(6) Smith, D. L. *Photogr. Sci. Eng.* **1974**, *18*, 309.
(7) Wiltberger, M.; Sharma, R.; Penner, T. L. *Langmuir* **1992**, *8*, 2639.
(8) West, W.; Gilman, P. B., Jr. *Photogr. Sci. Eng.* **1969**, *13*, 221.
(9) *The Theory of the Photographic Process*, 4th ed.; James, T. H., Ed.; Macmillan: New York, 1977.
(10) Wang, Y. *Chem. Phys. Lett.* **1986**, *126*, 209.
(11) Spano, F. C.; Mukamel, S. *Phys. Rev. A* **1989**, *40*, 5783.
(12) Ishimoto, C.; Tomimuro, H.; Seto, J. *Appl. Phys. Lett.* **1986**, *49*, 1677.
(13) Tani, T.; Suzumoto, T.; Kemnitz, K.; Yoshihara, K. *J. Phys. Chem.* **1992**, *96*, 2778.
(14) Muenter, A. A.; Brumbaugh, D. V.; Apolito, J.; Horn, L. A.; Spano, F. C.; Mukamel, S. *J. Phys. Chem.* **1992**, *96*, 2783.
(15) Herz, A. H.; Danner, R. P.; Janusonis, G. A. In *Adsorption from Aqueous Solution*; Weber, W. J., Jr., Matijevic, E., Eds.; ACS Monograph 79; Rheinhold: New York, 1968; p 173.
(16) Horng, M.; Quitevis, E. L. *J. Phys. Chem.* **1993**, *97*, 12408.
(17) Misawa, K.; Ono, H.; Minoshima, K.; Kobayashi, T. *Appl. Phys. Lett.* **1993**, *63*, 577.
(18) Sluch, M. I.; Vitukhnovsky, A. G.; Yonezawa, Y.; Sata, T.; Kunisawa, T. *Opt. Mater.* **1996**, *6*, 261.
(19) Rousseau, E.; Van der Auweraer, M.; De Schryver, F. C. *Langmuir* **2000**, *16*, 8865.
(20) De Feyter, S.; Hofkens, J.; Van der Auweraer, M.; Nolte, R. J. M.; Müllen, K.; De Schryver, F. C. *Chem. Commun.* **2001**, *7*, 585.
(21) Gaines, G. L., Jr. *Insoluble Monolayers at Liquid-Gas Interfaces*; Interscience: New York, 1966.
(22) Ulman, A. *Ultrathin Organic Films*; Academic Press: New York, 1991.
(23) Czikkely, V.; Försterling, H. D.; Kuhn, H. *Chem. Phys. Lett.* **1970**, *6*, 11.
(24) Buecher, H.; Kuhn, H. *Chem. Phys. Lett.* **1970**, *6*, 183.
(25) (a) Penner, T. L.; Moebius, D. *J. Am. Chem. Soc.* **1982**, *104*, 7407. (b) Vaidyanathan, S.; Patterson, L. K.; Moebius, D.; Gruniger, H. R. *J. Phys. Chem.* **1985**, *89*, 491. (c) Orrit, M.; Moebius, D.; Lehmann, U.; Meyer, H. *J. Chem. Phys.* **1986**, *85*, 4966.
(26) (a) Nakahara, H.; Moebius, D. *J. Colloid Interface Sci.* **1986**, *114*, 363. (b) Nakahara, H.; Fukuda, K.; Moebius, D.; Kuhn, H. *J. Phys. Chem.***1986**, *90*, 6144.
(27) Sugi, M.; Saito, M.; Fukui, T.; Iizima, S. *Thin Solid Films* **1985**, *129*, 15.
(28) Liu, M. H.; Kira, A.; Nakahara, H. *J. Phys. Chem.* **1996**, *100*, 20138.
(29) Yamaguchi, A.; Kometani, N.; Yonezawa, Y. *J. Phys. Chem. B* **2005**, *109*, 1408.
(30) (a) Hada, H.; Hanawa, R.; Haraguchi, A.; Yonezawa, Y. *J. Phys. Chem.* **1985**, *89*, 560. (b) Yonezawa, Y.; Möbius, D.; Kuhn, H. *Ber. Bunsen-Ges. Phys. Chem.* **1986**, *90*, 1183.
(31) Lehmann, U. *Thin Solid Films* **1988**, *160*, 257.
(32) (a) Saito, K.; Ikegami, K.; Kuroda, S.; Saito, M.; Tabe, Y.; Sugi, M. *J. Appl. Phys.* **1990**, *68*, 1968. (b) Saito, K.; Ikegami, K.; Kuroda, S.; Saito, M.; Tabe, Y.; Sugi, M. *J. Appl. Phys.* **1991**, *69*, 8291. (c) Saito, K.; Ikegami, K.; Kuroda, S.; Saito, M.; Tabe, Y. *J. Appl. Phys.* **1992**, *71*, 1401.
(33) Bliznyuk, V. N.; Kirstein, S.; Moehwald, H. *J. Phys. Chem.* **1993**, *97*, 569.
(34) Kirstein, K.; Steitz, R.; Garbella, R.; Möhwald, H. *J. Chem. Phys.* **1995**, *103*, 818.
(35) (a) Vranken, N.; Van der Auweraer, M.; De Schryver, F. C.; Lavoie, H.; Bélanger, P.; Salesse, C. *Langmuir* **2000**, *16*, 9518. (b) Vranken, N.; Van der Auweraer, M.; De Schryver, F. C.; Lavoie, H.; Salesse, C. *Langmuir* **2002**, *18*, 1641. (c) Vranken, N.; Foubert, P.; Köhn, F.; Gronheid, R.; Scheblybin, I.; Van der Auweraer, M.; De Schryver, F. C. *Langmuir* **2002**, *18*, 8407.
(36) (a) Tian, C. H.; Zoriniants, G.; Gronheid, R.; Van der Auweraer, M.; De Schryver, F. C. *Langmuir* **2003**, *19*, 9831. (b) Tian, C. H.; Liu, D. J.; Gronheid, R.; Van der Auweraer, M.; De Schryver, F. C. *Langmuir* **2004**, *20*, 11569.
(37) Ono, S.; Yao, H.; Matsuoka, O.; Kawabata, R.; Kitamura, N.; Yamamoto, S. *J. Phys. Chem. B* **1999**, *103*, 6909.
(38) Menger, F. M.; Keiper, J. S. *Angew. Chem., Int. Ed.* **2000**, *39*, 1906.
(39) Kirby, A. J.; Camilleri, P.; Engberts, J. B. F.; Feiter, M. C.; Nolte, R. J. M.; Soderman, O.; Bergsma, M.; Bell, P. C.; Fielden, M. L.; Rodríguez, C. L. G.; Guélf, P.; Kremer, A.; McGregor, C.; Perrin, C.; Ronsin, G.; van Eijk, M. C. P. *Angew. Chem., Int. Ed.* **2003**, *42*, 1448.
(40) Bell, P. C.; Bergsma, M.; Dolbnya, I. P.; Bras, W.; Stuart, M. C. A.; Rowan, A. E.; Feiters, M. C.; Engberts, J. B. N. *J. Am. Chem. Soc.* **2003**, *125*, 1551.
(41) Jennings, K. H.; Marshall, I. C. B.; Wilkinson, M. J.; Kremer, A.; Kirby, A. J.; Camilleri, P. *Langmuir* **2002**, *18*, 2426.
(42) Chen, X.; Wang, J.; Shen, N.; Luo, Y.; Li, L.; Liu, M.; Thomas, R. K.; *Langmuir* **2002**, *18*, 6222.
(43) (a) Zhai, X.; Zhang, L.; Liu, M. *J. Phys. Chem. B* **2004**, *108*, 7180. (b) Zhai, X.; Liu, M. *J. Colloid Interface Sci.* **2006**, *295*, 181.
(44) Jiang, M.; Zhai, X.; Liu, M. *Langmuir* **2005**, *21*, 11128.
(45) Spitz, C.; Dähe, S.; Ouart, A.; Abraham, H. W. *J. Phys. Chem. B* **2000**, *104*, 8664.
(46) Yuan, J.; Liu, M. *J. Am. Chem. Soc.* **2003**, *125*, 5051.
(47) (a) Knapp, E. W. *Chem. Phys.* **1984**, *85*, 73. (b) Knapp, E. W.; Scherer, P. O. J.; Fisher, S. F. *Chem. Phys. Lett.* **1984**, *111*, 481.
(48) Honda, C.; Hada, H. *Tetrahedron Lett.* **1976**, 177. Honda, C.; Hada, H. *Photogr. Sci. Eng.* **1977**, *21*, 91.
(49) Ribó, J. M.; Crusats, J.; Sagués, F.; Claret, J.; Rubires, R. *Science* **2001**, *292*, 2063.
(50) Zhang, L.; Lu, Q.; Liu, M. *J. Phys. Chem. B* **2003**, *107*, 2565. Zhang, L.; Yuan, J.; Liu, M. *J. Phys. Chem. B* **2003**, *107*, 12768.
(51) *Circular Dichroism Principles and Applications*, 2nd ed.; Berova, N., Nakanishi, K., Woody, R. W., Eds.; Wiley-VCH: New York, 2000.
(52) Rabe, J. P.; Buchholz, S. *Phys. Rev. Lett.* **1991**, *66*, 2096.
(53) Boehringer, M.; Schneider, W. D.; Berndt, R. *Angew. Chem., Int. Ed.* **2000**, *39*, 792.
(54) Li, C. J.; Zeng, Q. D.; Wang, C.; Wan, L. J.; Xu, S. L.; Wang, C. R.; Bai, C. L. *J. Phys. Chem. B* **2003**, *107*, 747.